Improving the understanding of N transport in a rural catchment under Atlantic climate conditions from analysis of the concentration-discharge relationship derived from a high frequency data set

Rodríguez-Blanco, María Luz[1], Taboada-Castro, María Mercedes[2], Taboada-Castro, María Teresa[3]

[1]History, Art and Geography Department, GEAAT Group, University of Vigo, Campus As Lagoas, 36310 Ourense, Spain
[2]ETSIIAA, Area of Soil Science and Soil Chemistry, University of Valladolid, 34004 Palencia, Spain
[3]Faculty of Sciences, Centre for Advanced Scientific Research (CICA), University of A Coruna 15071 A Coruña, Spain

Correspondence to: M.L. Rodríguez-Blanco (maria.luz.rodriguez.blanco@uvigo.es)

Abstract. Understanding processes controlling stream nutrient dynamics over time is crucial for implementing effective management strategies to prevent water quality degradation. In this respect, the study of the nutrient concentration-discharge (C-Q) relationship during individual runoff events can be a valuable tool for extrapolating the hydrochemical processes controlling nutrient fluxes from streams. This study investigated nitrogen concentration dynamics during events by analysing and interpreting the nitrogen C-Q relationship in a small Atlantic (NW Iberian Peninsula) rural catchment. To this end, nitrate (NO_3^-) and total Kjeldahl nitrogen (TKN) concentrations were monitored at high temporal resolution during 102 runoff events over a 6-year period. For each of the selected runoff events, C-Q response was examined visually for the presence and direction of hysteresis loops and classified into three types of responses: clockwise and anticlockwise and no hysteresis. Change in concentration (ΔC) and the dynamics of hysteresis loops (ΔR) were used to quantify nitrogen (NO_3^- and TKN) patterns during the runoff events. The transport mechanisms varied between elements. The most frequent hysteretic response for NO_3^- was enrichment with anticlockwise rotation. On the contrary, the TKN dynamic was dominated enrichment with clockwise hysteresis. Hysteresis direction (ΔR) and magnitude (ΔC) for TKN were better explained by event characteristics, such as rainfall, peak discharge, and event magnitude than by antecedent conditions (antecedent precipitation and baseflow). For NO_3^- hysteresis the role of hydrometeorological conditions were more complex. NO_3^- hysteresis magnitude (ΔC) was related to the magnitude of the event (ΔQ) and the time elapsed since a preceding runoff event (Δt). These findings could be used as a reference for the development of N mitigation strategy in the region.

Keywords: concentration-discharge, hysteresis, nitrogen, runoff events, rural catchment, Atlantic climate, NW Iberian Peninsula.

1 Introduction

Increasing nitrate concentrations in headwater catchments is a pressing environment issue (EEA, 2018; Musolff et al., 2018; Koening et al., 2021). In Europe, despite the advances made in the field of improving the quality of water bodies in recent decades, 60% of freshwaters fail to achieve good ecological status as established by the Water Framework Directive (Directive

2000/60/EC) (EEA, 2018). The European Directive urges Member States to monitor water quality. However, many Member States, Spain among them, have an inadequate water monitoring network to ensure a comprehensive and consistent monitoring

35   of water bodies (EC, 2019). Water quality assessments historically have relied on routine low-frequency monitoring at main rivers, commonly every two weeks or at monthly resolution. This traditional sampling method can provide valuable information to identify sites that are under pressure due to anthropogenic activities, also to observe long-term trends in relation to land use but cannot provide knowledge on nutrient dynamics under contrasting hydrological condition (Dupas et al., 2016; Rose et al., 2018a; Musolff et al., 2021), which is essential to develop suitable management programs to restore or maintain

40   water quality (Lloyd et al., 2016; Bieroza et al., 2018).

One way of approaching the study of nutrient dynamics involves analysing the nutrient concentrations and discharge (C-Q) relationship at a given point in the stream during runoff events (Bieroza and Heathwaite, 2015; Lloyd et al., 2016; Rose et al., 2018; Baker and Showers, 2019), which requires high-frequency measurements of concentration and discharge. The most observed pattern in the C-Q relationship is the hysteresis loop, which reflects a non-linear solute or particulate behavior during

45   runoff events as concentrations at a given discharge differ on the rising and falling limb of the hydrograph (Williams, 1989; Evans and Davies, 1998). The width, magnitude and direction of these loops have been used to investigate the sources, flow paths and transport mechanisms responsible for the export of nutrients from catchments (Evans and Davies, 1998; Butturini et al., 2008; Dupas et al., 2016; Vaughan et al., 2017; Barros et al., 2020). Hysteresis -C-Q relationships are classified into clockwise and anticlockwise according to their direction (Figure 1). Generally, clockwise hysteresis is interpreted to reflect

50   proximal and rapidly mobilized sources, whereas anticlockwise hysteresis reflects sources that are either proximal to the stream channel with slow transport, or those that are distal to the stream (Williams, 1989; Lloyd et al., 2016; Baker and Showers, 2019; Knapp et al., 2020; Evans and Davies, 1998). Complex hysteresis loops are often the result of the spatial-temporal variability of rainfall, antecedent moisture conditions, etc. (Ramos et al., 2015). The C-Q relationship can also result in positive or negative hysteresis slopes representing enrichment or dilution effects, respectively (Butturini et al., 2008; Lloyd et al., 2016;

55   Vaughan et al., 2017).

Numerous studies have examined the nitrogen, particularly nitrate (NO_3^-), C-Q relationship at event scale in varying sizes of catchments under different degrees of human impact (e.g., Butturini et al., 2008; Cerro et al., 2014; Dupas et al., 2016; Outram et al., 2016; Vaughan et al., 2017; Baker and Showers, 2019; Musolff et al., 2021; Winter et al., 2021), showing evidence of diverging C-Q relationship in agricultural and forest catchments. For example, in intense agricultural management catchments

60   NO_3^- showed consistent response between events, dominated by clockwise enrichment or dilution patterns (Cerro et al., 2014; Dupas et al., 2016; Outram et al., 2016). In the case of forested catchments, where NO_3^- response was highly variable, NO_3^- enrichment C-Q pattern with clockwise or anticlockwise hysteresis prevailed (Vaughan et al., 2017; Musolff et al., 2021). Hysteresis patterns can change from one runoff event to another and several factors as such antecedent wetness conditions, event characteristics as well as event-water contributions play an important role in controlling the variability in NO_3^- C-Q

65   relationship among different hydrological events (Outram et al., 2016; Baker and Showers, 2019; Knapp et al., 2020). For example, Knapp et al. (2020) observed dilution behaviour during wetter conditions and stronger mobilization following drier
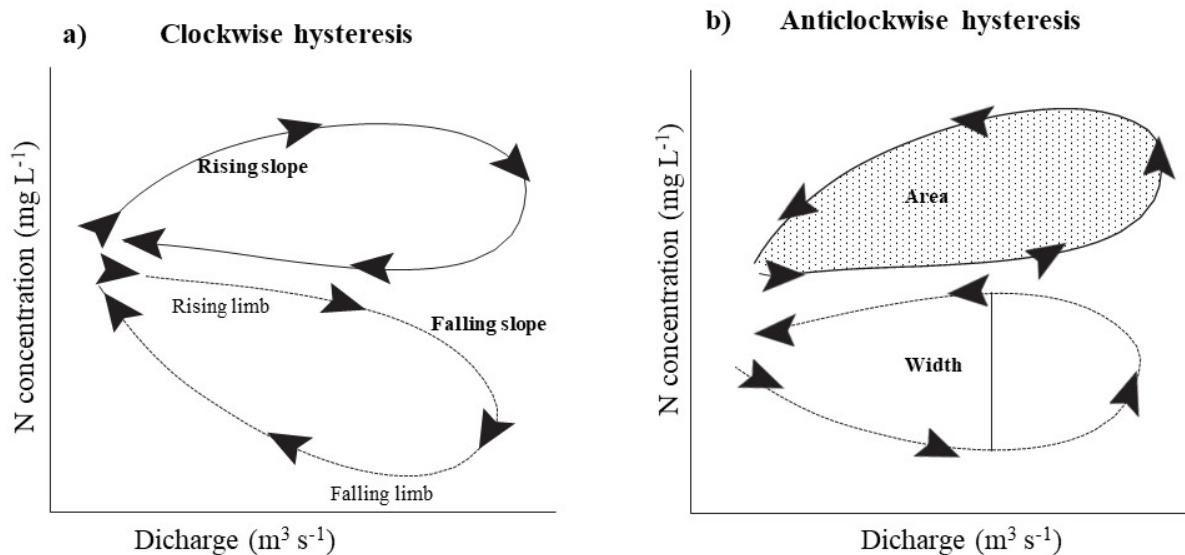
Figure 1: Idealized representation of (a) clockwise and (b) anticlockwise hysteresis loops, showing that each pattern can occur with either enrichment or dilution during the rising limb of the hydrograph. The loop width and area are shown in panel b.

70   conditions and during events with larger event-water contributions. However, others found that NO_3^- hysteresis behaviour was better explained by runoff event magnitude and rainfall intensity (Butturini et al., 2008; Aguilera and Melack, 2018) . Comparatively, approaches for the analysis of organic N C-Q relationship at the event scale are scarce and when exist focus mostly on organic dissolved nitrogen (e.g., Kaushal and Lewis, 2003; Chen et al., 2012; D'Amario et al., 2021). The literature suggests that even though dissolved organic nitrogen accounts for only a portion of the nitrogen in streams draining in

75   agricultural management catchments, both particulate and dissolved forms of organic nitrogen can constitute a significant portion of the total nitrogen export in rural and forested catchments (Hagedorn et al., 2000; Kaushal and Lewis, 2003; Aguilera and Melack,2018). Therefore, the analysis of NO_3^- and total organic nitrogen C-Q relationships may provide useful information about the processes regulating N transport though the landscape. So far, studies integrating both NO_3^- and total organic nitrogen C-Q relationships into a coherent framework in the Southwest of Europe are scarce, partly due to the limited availability of

80   high-frequency data. This information is essential to anticipate changes in freshwater resources in compliance with the Water Framework Directive planning and monitoring norms. Therefore, it is necessary to provide new information on the issue to augment current studies across Europe and the Iberian Peninsula, in particular.

In this context, the aim of this study was to understand differences in the behaviour of NO_3^- and total Kjeldahl nitrogen (TKN) concentrations. For this, we used high-frequency measurements of NO_3^- and TKN concentration obtained during runoff events

85   of contrasting magnitudes at the outlet of an Atlantic headwater catchment localized in NW Iberian Peninsula. More specifically the study aims to explore questions such as i) how NO_3^- C-Q behaviour differs from that of TKN C-Q; ii) how variable C-Q relationship between individual events are; and iii) whether variability in C-Q relationships can be explained by

specific rainfall-runoff event characteristics, such as antecedent wetness conditions, rainfall, runoff volume, etc. The selected catchment (Corbeira, 16 km^2, NW Iberian Peninsula) is of particular interest, as it is a tributary of the Mero River, which discharges into the Abegondo-Cecebre reservoir - the main water supply for the city of A Coruña and surrounding municipalities (450 000 inhabitants) - and finally drains into the Atlantic Ocean through the ria of O Burgo. The Cecebre-Abegondo reservoir is a Natural 2000 EU site, classified as a Special Area of Conservation (ES1110004) in 2014 under the EU Habitats Directive (Directive 92/43/ECC) and one of the Core Zones of the Mariñas Coruñesas e Terras do Mandeo Biosphere Reserve, sustaining important bird, macroinvertebrate, and fish populations. Nevertheless, the ecological status of the Abegondo-Cecebre reservoir has deteriorated in the last few decades due to pollution, the presence of invasive alien species and fluctuations of river flow discharge (Ameijenda et al., 2010).

2 Material and methods

2.1 Study site

The study was conducted in a headwater catchment of 16 km^2 located in NW Spain, approximately 30 km southeast of the city of A Coruña (Galicia, NW Iberian Peninsula) (Figure 2). The catchment is characterized by low drainage density (1.38 km km^{-2}), mean slope of 19% and a maximum altimetric amplitude of 410 m (675-65 m). The bedrock consists of basic schist of the Órdenes Complex (IGME, 1981) and the soils are predominantly Umbrisols and Cambisols (IUSS, 2015), with a silt and silty-loam texture, variable organic matter content (4.4-10.5%) and acid pH in the surface soil layer. The soils have a high infiltration capacity, so overland flow is unusual. Groundwater is the dominant source of water to the stream and the baseflow index is 0.75 (Rodríguez-Blanco, et al., 2012a). The catchment land cover consists of a mixture of forest (65%), agricultural fields (30%) and impervious areas (5%), consisting of roads and single-family homes that are not always connected to sewage disposal systems. Agricultural areas are dominated by pastures (26% of total area), the remaining agricultural area (4%) cultivates maize and winter cereals. Organic and inorganic fertilizers are commonly used in agricultural areas throughout the year, including the wettest months. Forest areas are not fertilized. The annual N input to the catchment is approximately 37.8 kg N ha^{-1} (Rodríguez-Blanco et al., 2015), so nitrogen inputs in the Corbeira catchment can be considered low when compared to catchments with more intense agriculture.

The study area is located within the Eurosiberian biogeographic region, particularly in the Cantabrian-Atlantic province (Instituto Geográfico Nacional, 2008). It is included in the temperate oceanic climate region (Csb) according to Köppen-Geiger classification. Mean annual rainfall and temperature for the period 1983-2020 are 1075 mm and 13ºC, respectively (data from the station ID 10045 of the official meteorological service of the Galician Government-Meteogalicia, located near to the study catchment). The wettest period is from October to March, and the driest and hottest months are usually in summer (June-September). The hydrological regime is pluvial oceanic, with maximum discharge in December and low flows from June to September. Mean daily-recorded discharge is 0.18 m3 s-1. For more detailed information of the hydrological behaviour of this catchment see (Rodríguez-Blanco et al., 2012b; 2020).
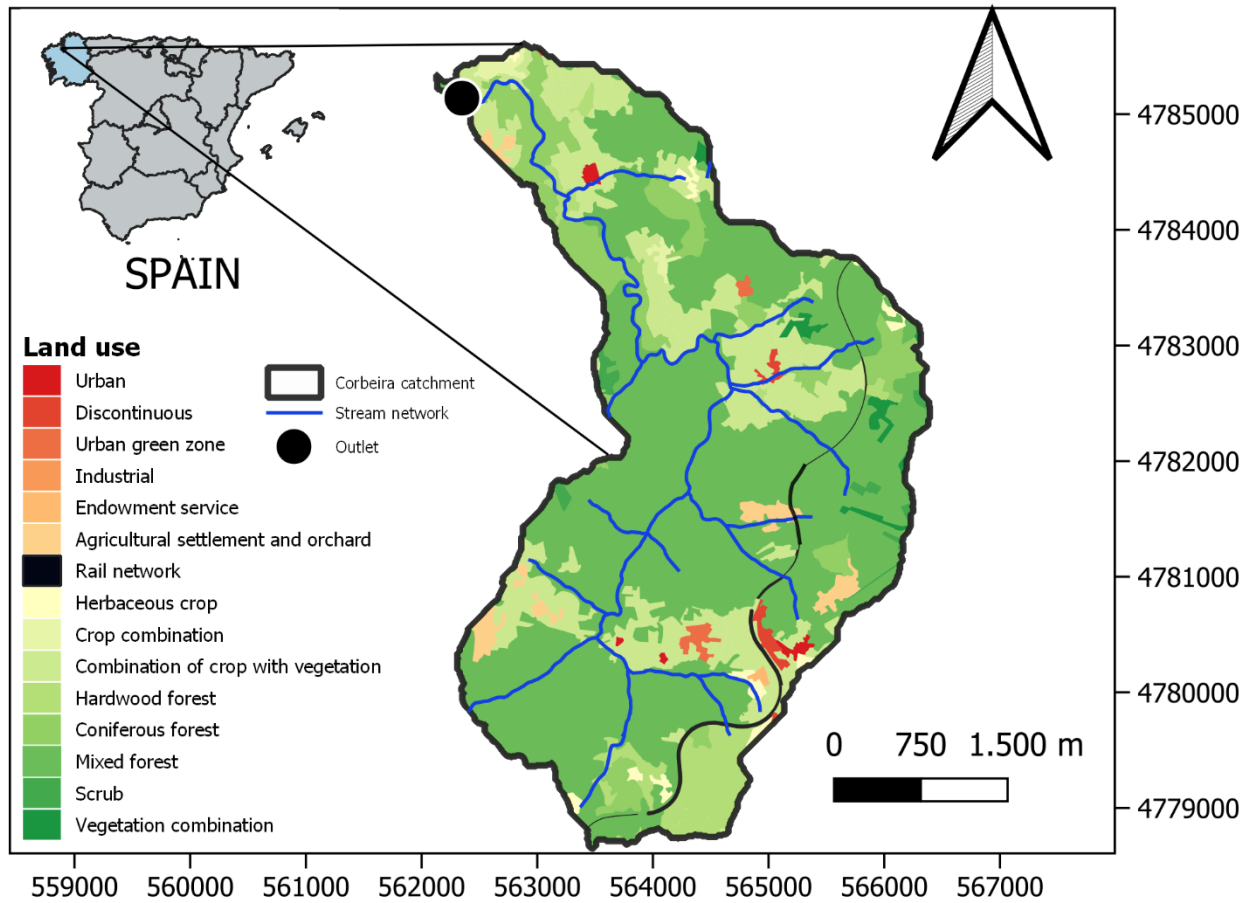
Figure 2: Location and land use of the Corbeira catchment.

2.2 Data acquisition: monitoring, sampling, and water analysis

The research period comprised six hydrological years (1st October to 30th September), during which rainfall, discharge, and N (NO_3^- and TKN) concentrations were measured. Rainfall was monitored at 10-min intervals using three rainfall gauges (0.2 mm resolution) distributed across the catchment. The Thiessen Polygon method (Linsey et al., 1949) was used to calculate the mean rainfall in the catchment. Water discharge was obtained at 10-min resolution at the catchment outlet. Stream water level was measured with a differential pressure transducer sensor (ISCO-720) coupled to an automatic water sampler (ISCO 6712-FS) at 1 min intervals and recorded at 10-min resolution. The water level was then converted into discharge by rating-curve development over a wide range of discharge conditions at the sampling location.

Stream water samples were taken at the catchment outlet during runoff events using the automatic water sampler (Teledyne ISCO, Portable Sampler 6712-FS) fitted with 24 polypropylene 1-liter bottles. The pump inlet of the autosampler was placed near the pressure sensor. The sampler was programmed to start when the stream water level increased 2-3 cm above the level at the beginning of a rainfall event, and water samples were taken at fixed intervals (1-8 h) during the rising and recession limbs of the hydrograph to collect key runoff phases. The pumping frequency was modified manually depending on the expected magnitude and duration on runoff events based on weather forecasts together with the experience accumulated from water sampling over the years. Samples were removed from the autosampler within a few hours after runoff events and transported to the laboratory where they were stored in the dark and refrigerated at 4ºC until analysed for the following parameters: electrical conductivity (EC), ammonium (NH_4^+), total Kjeldahl nitrogen (TKN), nitrate (NO_3^-) and nitrite (NO_2^-); NH_4^+ was only analysed during the first six months of the study. Electrical conductivity at a reference temperature of 20 ºC was measured using a Crison conductivity meter. TKN concentrations were determined by Kjeldahl digestion of unfiltered samples according to the APHA method (APHA, 1998). After sample filtration (0.45 μm) NO_3^- and NO_2^- concentrations were analysed by capillary electrophoresis, while NH_4 was measured using an ammonia-selective electrode. In this paper, only data concerning NO_3^- and TKN are presented because the concentrations of NO_2^- and NH_4^+ measured were below the detection limit (0.06 and 0.05 mg L^{-1}, respectively).

2.3 Selection of runoff events and description of C-Q hysteresis

The runoff events were defined as any hydrological response to rainfall events which resulted in discharge increase equal to or higher than 1.5 times the discharge at the beginning of a rainfall event (the latter being defined as a rainfall episode, usually exceeding 5 mm of rainfall, following an interval of at least 10 hours with no rain). For each runoff event, the stream discharge was separated into two components (direct runoff and baseflow) using the constant slope hydrograph separation method of Hewlett and Hibbert (1967) and a constant slope of 1.83 L s^{-1} km^{-2} d^{-1}, as suggested in other Spanish forested catchments (e.g., Latron et al., 2008). It was assumed that a runoff event begins when a perceptible increase in discharge was observed and ends when discharge returned to baseflow conditions or when another hydrological event commenced (Figure 3).

The events were characterized by three groups of variables which were hypothesized as potential controls on the N dynamic due their influence on the hydrológical response of the catchment (Rodríguez-Blanco et al., 2012): i) variables related to antecedent wetness conditions (i.e., variables characterizing the conditions prior to the event), ii) event variables (rainfall and discharge) and iii) variables related to NO_3^- and TKN concentrations (Table 1). Antecedent wetness conditions were described by accumulated rainfall 7 and 15 days prior to the event (AP7d, and AP15d, respectively, mm), the discharge at the beginning of the event (Q_b, m^3 s^{-1}) and the time from the previous runoff event (Δt, h). Event variables included rainfall amount (P, mm); maximum 10-min rainfall intensity (IP10, mm h^{-1}); rainfall kinetic energy (KE, MJ ha^{-1}) determined according to the Wischmeier and Smith (1958); peak discharge (Q_{max}, m^3 s^{-1}); water yield (WY, mm), i.e. total water volume during the runoff event (direct runoff +baseflow); magnitude of the event relative to the initial baseflow (ΔQ; i.e., $(Q_{max}-Q_b)/Q_b*100$, %);

relative length of the rising limb (RL, %) given by $RL=R_D/S_D *100$ where R_D and S_D are the length (h) of the rising limb of the hydrograph and of the entire hydrograph, respectively; slope of hydrograph falling limb (k, 1/day) and runoff event duration (Rd, h). Finally, to describe NO_3^- and TKN concentrations, the initial, maximum, and discharge-weighted mean concentrations of NO_3^- and TKN measured during the events were included $NO_3C_{initial}$, NO_3C_{max}, NO_3C_{mean}, $TKNC_{initial}$, $TKNC_{max}$, $TKNC_{mean}$, respectively; mg L^{-1}). The discharge-weighted mean concentration of the event was computed as total load divided by the total flow.
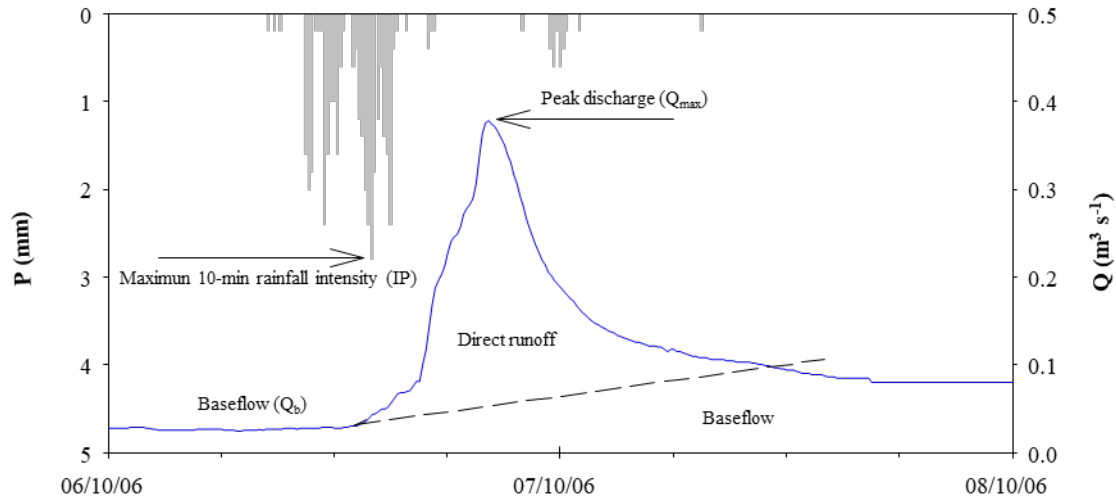
Figure 3: Diagram illustrating the hydrograph separation in two components (direct runoff and baseflow) using the constant slope hydrograph separation of Hewlett and Hibbert (1967). Some variable characteristics of the rainfall-runoff events are also indicated.

During the entire monitoring period, 173 runoff events were identified; 156 were sampled, the other 17 were missed because of technical problems with the equipment. In total, 102 events of varying magnitude and duration were selected for C-Q analysis in this study. Following the methodology of Rodríguez-Blanco et al. (2017), selection criteria used for hysteresis analysis of runoff events were that they had to have only one peak discharge with at least two samples collected on each limb of the hydrograph, and one sample at or close to peak discharge, because this was considered the minimum number of samples from which rotational direction could be identified. For each of the selected runoff events, C-Q NO_3^- and TKN response were verified visually for the presence and direction of a hysteresis loop (by plotting concentration versus discharge) and classified into three types of responses: clockwise, anticlockwise and no hysteresis. Events with a "figure-eight" hysteresis pattern were classified as a hysteresis response, with the direction depending on the succession of the peak concentration and peak discharge (i.e., clockwise, or anticlockwise), in a similar way to Bieroza and Heathwaite (2015).

Table 1. Characteristics of the runoff events (n=102) selected during the study. CV: Coefficient of variation.

Variable		Mean	Minimum	Maximum	CV (%)
Antecedent conditions	Accumulated rainfall 7 days before the event (AP7d, mm)	35.18	0.60	124.40	81
	Accumulated rainfall 15 days before the event (AP15d, mm)	67.29	1.00	222.10	77
	Discharge at the beginning of the event (Qb, m^3 s^{-1})	0.21	0.03	0.64	60
	Time from the previous runoff event (Δt, h)	236.83	0.00	4065.02	212
Event conditions	Rainfall amount (P, mm)	22.24	4.00	74.40	69
	Maximum 10-min rainfall intensity (IP10, mm h^{-1})	2.35	0.40	9.20	71
	Rainfall kinetic energy (KE, MJ ha^{-1})	3.16	0.52	10.49	74
	Peak discharge (Qmax, m^3 s^{-1})	0.49	0.10	1.62	65
	Water yield (WY, mm)	40711.68	4097.01	190026	99
	Magnitude of the event (ΔQ, %)	165.57	17.65	853.33	92
	Relative length of the rising limb (RL, %)	33.63	11.63	64.35	38
	Slope of the initial phase of the hydrograph falling limb (k, 1/day)	-0.016	-0.053	-0.001	72
	Runoff event duration (Rd, h)	32.41	9.80	115.80	59
TKN and NO$_3$ concentrations during the events	*NO$_3^-$*				
	Initial concentration (NO3C$_{initial}$, mg L^{-1})	5.41	3.11	12.61	27
	Maximum concentration (NO3C$_{max}$, mg L^{-1})	7.09	3.14	22.51	41
	Mean concentration (NO3C$_{mean}$, mg L^{-1})	5.84	3.12	10.06	25
	TKN				
	Initial concentration (TKNC$_{initial}$, mg L^{-1})	0.25	0.01	2.55	129
	Maximum concentration (TKNC$_{max}$, mg L^{-1})	1.47	0.08	9.41	96
	Mean concentration (TKNC$_{mean}$, mg L^{-1})	0.6375	0.04	2.88	79
Hysteresis descriptors	*NO$_3^-$*				
	Hysteresis direction (ΔR, %)	-20.62	-93.00	60.00	151
	Hysteresis magnitude (ΔC, %)	3.86	-44.28	47.20	395
	TKN				
	Hysteresis direction (ΔR, %)	4.78	-72.00	69.00	513
	Hysteresis magnitude (ΔC, %)	66.15	-70.35	98.45	61

Following the methodology proposed by Butturini et al. (2006) the form, rotational patterns, and slope of NO$_3^-$ and TKN hysteresis loops were characterised by two descriptors: hysteresis magnitude (ΔC, %) and hysteresis direction (ΔR, %). Hysteresis magnitude (ΔC) describes the relative changes in nitrogen (NO$_3^-$ or TKN) concentration and hysteresis slope, and is calculated using the following equation:

$$\Delta C \begin{cases} \frac{Cs-Cb}{Cmax} * 100 \text{ if } Cs > Cb \\ \frac{Cs-Cb}{Cb} * 100 \text{ if } Cs < Cb \end{cases} \quad (2)$$

where C_s and C_b are the nitrogen (NO_3^- or TKN) concentrations at peak discharge and baseflow, respectively, and C_{max} is the highest concentration measured in the stream during the runoff event. ΔC ranges from - 100 to 100%, where positive values indicate hysteresis loops following a positive slope with respect to the discharge, i.e., element flushing, and negative values indicate the opposite, i.e., solute dilution. Hysteresis direction (ΔR) reflects the entire element dynamics during runoff events and provides information on the area (magnitude) and rotational (direction) pattern of the C-Q hysteresis. ΔR is calculated by the following equation:

$$\Delta R = R * Ah * 100 \tag{3}$$

where Ah is the area of the C-Q hysteresis, estimated after standardizing discharges and concentrations to unit on dividing nitrogen (NO_3^- or TKN) concentrations and discharge by their peak values and the calculating the area under the loop. Thus, Ah takes values between 0 and 1; the closer to zero the Ah value, the more linear is the loop, indicating no significant difference in nitrogen (NO_3^- or TKN) concentrations between the rising and falling limbs. On the contrary, an Ah value close to 1 indicates that the area of the hysteresis loop is large, showing significant differences in nitrogen (NO_3^- or TKN) concentrations in both limbs of the hydrograph at similar discharge. R describes the rotational pattern of the hysteresis. If the C-Q hysteresis is clockwise, R=1, and if it is anticlockwise, R=-1; for ambiguous or non-existent hysteresis, R=0. The descriptor ΔR also varies from -100 to 100 %.
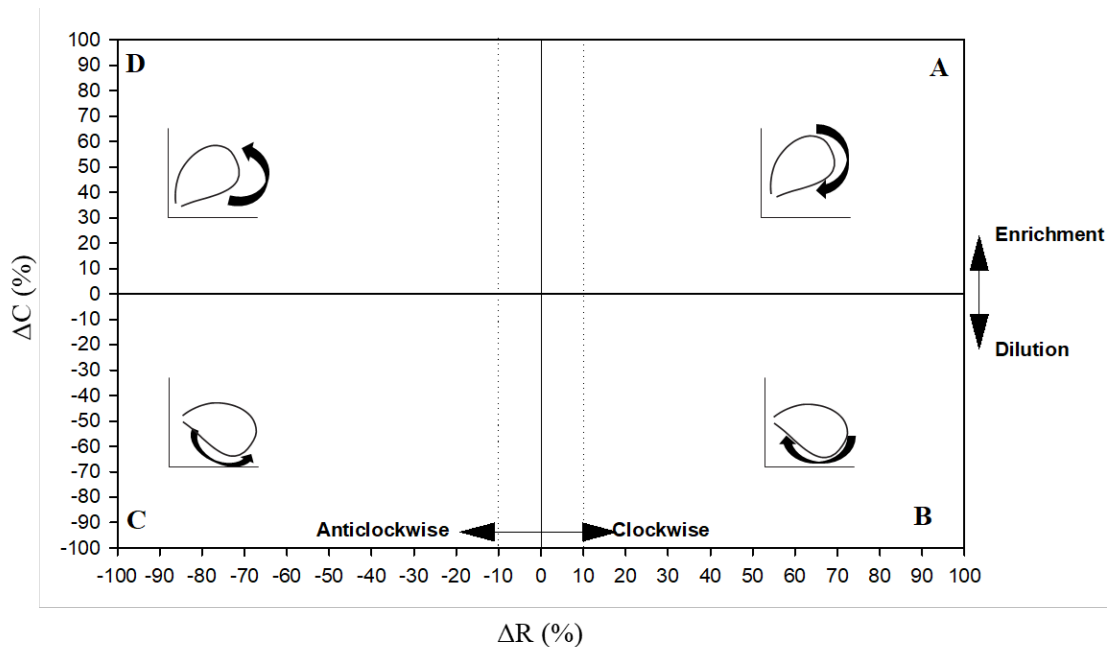
Figure 4: Schematic representation of the ΔC versus ΔR showing different forms of C-Q relationships. The vertical dotted lines delimit hysteresis loops with small area. Circular arrows show the direction of clockwise and anticlockwise hysteresis. Own elaboration based on Butturini et al. (2006).

The variability of NO_3^- and TKN hysteresis descriptors was examined by plotting hysteresis magnitude (ΔC) versus hysteresis
rotation (ΔR). The plots can be divided in 4 zones (Butturini et al., 2006), each of which identifies a C-Q response type (Figure
4). For this, ΔC and ΔR descriptors were classified in two distinct categories ("-1", "1"): $\Delta C < 0$ (element dilution); $\Delta C > 0$
(element release); $\Delta R < 0$ (anticlockwise loop); $\Delta R > 0$ (clockwise loop). Hysteresis with ΔR values from -10 to 10% were
considered to have small area.

2.4 Statistical methods

To assess the main links between hysteresis descriptors (response variables) and the different hydro-meteorological and
biogeochemical variables (explanatory variables) influencing these events, standard statistical methods were used, such as
correlation (Pearson correlation coefficient) and a redundancy analysis (RDA). RDA is an extension of multiple regression
that models the effects of explanatory variables on response variables assuming linear relationships (Legendre and Legendre,
2012). The RDA output was represented in a biplot graph showing the correlation between explanatory and response variables
given by the cosine of the angle between vectors. Thus, vectors pointing in roughly the same direction represent a positive
correlation, while those pointing in opposite directions show a negative correlation.

3 Results

3.1 Average characteristics of the rainfall-runoff events

The main characteristics of the runoff events selected for this study are summarized in Table 1. High variability in the variables
defining the events was observed. Thus, the events varied greatly in terms of antecedent conditions (AP7d: 0.60 - 124.40 mm,
AP15d: 1.00 - 222.10 mm, Q_b: 0.03 - 0.64 $m^3 s^{-1}$), meteorological (P: 4.00 -74.40 mm, KE: 0.52 - 10.49 MJ ha^{-1}) and
hydrological features (Q_{max}: 0.10 - 1.62 $m^3 s^{-1}$, ΔQ: 17.65 - 853.33%, Rd: 9.80 - 115.80 h), showing that those selected cover
a wide range of meteorological and hydrological conditions. These events (i.e., the 102 used in the study) can be considered
representative of the rainfall-runoff event characteristics of the study period, because the meteorological and hydrological data
of the events in this study are within the 5th to 95th percentile range of rainfall, antecedent rainfall and discharge of the events
occurring in the area during the study period.
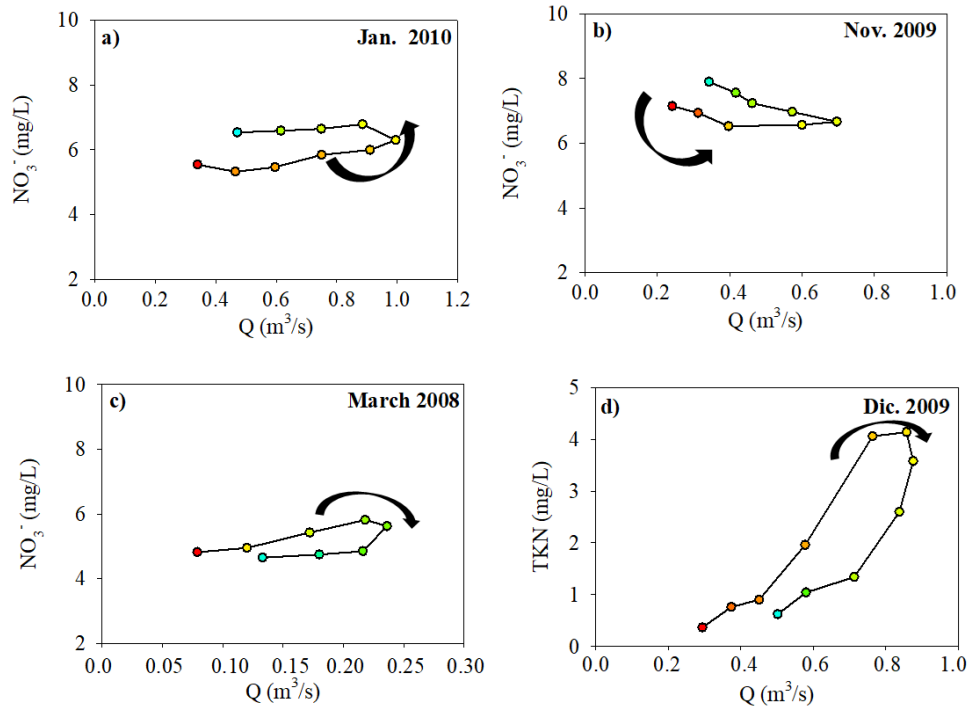
Figure 5: Examples of different types of NO$_3^-$ (a, b and c) and TKN (d) hysteresis patterns observed in the Corbeira catchment during the monitoring period, where red colors indicate the start of the runoff event and blue colors the end of the runoff events. (a) Enrichment with anticlockwise pattern, (b) Dilution with anticlockwise pattern, (c and d) Enrichment with clockwise pattern Circular arrows show the direction of clockwise and anticlockwise hysteresis.

From the selected 102 rainfall-runoff events, 39 occurred in autumn, 30 in winter, 22 in spring and 11 in summer, so that about 70% were concentrated in the wettest period of the year (October-March). The magnitude of the runoff events tended to be high in autumn and winter when soil moisture is high, while in summer, when the catchment is dryer, the event magnitude tended to be lower (Rodríguez-Blanco et al., 2012a) (Figure 5c). In the study area, the runoff events are usually linked to low-magnitude (mean P = 22.24 mm) and intensity (mean IP10 = 2.35 mm h^{-1}) rainfall events of long duration (mean 14.8 h, data not shown), although several with high magnitude (P > 50 mm) and intensity (IP 10 = 9.1 mm h^{-1}) rainfall were registered during the study (Table 1). For most runoff events, an increase in NO$_3^-$ and TKN concentrations with discharge were observed, but the magnitude of the increase varied markedly from one event to another. The mean and maximum N (NO$_3^-$ and TKN) concentrations also varied among runoff events, especially for TKN; the maximum TKNC$_{mean}$ and TKNC$_{max}$ values were two orders of magnitude higher than the respective minimum values (Table 1). The highest values of both elements were recorded during autumn events (Figure 5).

3.2 Hysteresis direction and magnitude

The study of the relationship between the N (NO_3^- and TKN) concentration and discharge revealed different hysteresis patterns
255   for both elements in the catchment (Figure 5 and 6). For NO_3^-, the parameter describing the change in concentration during
the runoff events returned positive values ($\Delta C \geq 0\%$) in 64 events. These positive values show that NO_3^- concentrations during
the runoff events were mostly greater than before the event; but 35 of these events had ΔC values between 0% and 10%,
indicating small increase in NO_3^- concentrations (Butturini et al., 2008).

Based on hysteresis classification, 74% of the events exhibited anticlockwise hysteresis ($\Delta R < 0$), 21% clockwise hysteresis
260   ($\Delta R > 0$) and the remaining 5% showed no or unclear hysteresis pattern ($\Delta R = 0$). However, it should be noted that
approximately 13% of events had ΔR values between -10% and 10%, so in these cases it is considered that the hysteresis area
is small. NO_3^- data are in all areas in the ΔC *vs.* ΔR unit plane (Figure 6 up), although the hysteresis loops are located mainly
in zones D and C (Figure 6 top), indicating dilution (negative ΔC) or flushing (positive ΔC) and anticlockwise hysteresis loops
(negative ΔR).

265   TKN concentrations increased in almost all runoff events compared with pre-event values (positive ΔC in 93% of events),
indicating that TKN flushing clearly predominates over dilution. In fact, the parameter describing the change in concentration
during runoff events (ΔC) achieved negative values in only 7 runoff events (Figure 6 bottom), all of which were characterized
by low rainfall. The rotational patterns of the TKN-Q hysteresis ranged from clockwise ($\Delta R > 0$) to anticlockwise ($\Delta R < 0$)
(Figure 6 bottom). About 53% of the events showed clockwise hysteresis, 39% anticlockwise hysteresis and the remaining 8%
270   showed no or unclear hysteresis pattern; although it should be noted that 29% of the events showed small areas of the hysteresis
loop (ΔR values stood between -10% and 10%). The hysteresis loops are located mainly in the zones A and D (Figure 6
bottom), suggesting a flushing (positive ΔC) and clockwise (positive ΔR) or anticlockwise loops (negative ΔR).
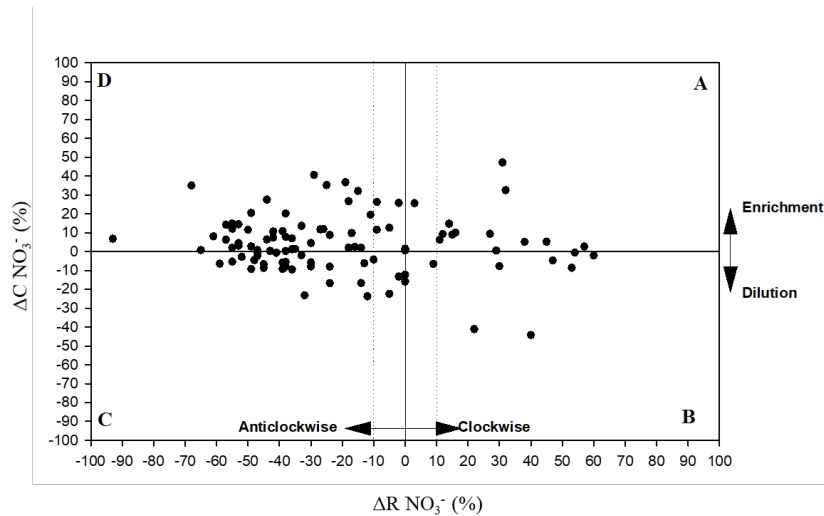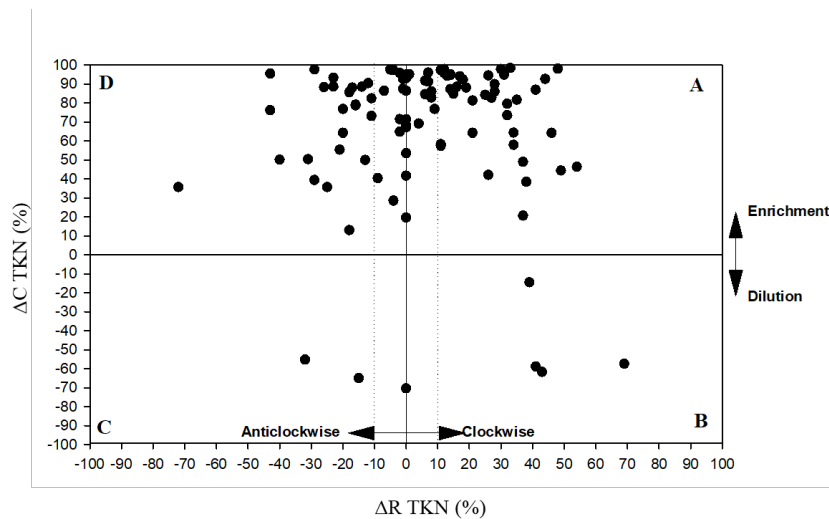
Figure 6: Representation of the C-Q hysteresis characteristics (ΔR, ΔC) of NO_3^- (up) and TKN (bottom) in the unity plane. The vertical and horizontal dotted lines delimit hysteresis loops of small area.

275

3.3 C-Q hysteresis response controls

To identify the variables that might explain C-Q hysteresis patterns the relationships between hysteresis descriptors and hydrological and biogeochemical variables were analyzed using a Pearson correlation matrix and an RDA analysis (Table 2 and Figure 7). The results of the correlation analysis showed that the hysteresis direction and magnitude were more closely
280 related to certain event characteristics than antecedent conditions (Table 2). Thus, of the representative variables of the event antecedent conditions, significant correlations (negative sign) were observed between the discharge at the beginning of the event (Q_b), and time from the previous runoff event (Δt) and the hysteresis magnitude parameter for NO_3 (r = -0.22, p < 0.05). The parameter describing information on the hysteresis direction for NO_3 (ΔR_{NO3}) showed negative correlations with rainfall amount (P), maximum 10-min rainfall intensity (IP10), rainfall kinetic energy (KE) and peak discharge (Q_{max}). On the contrary,
285 a positive relationship was found between hysteresis direction for TKN (ΔR_{TKN}) and rainfall amount (P), maximum 10-min rainfall intensity (KE), peak discharge (Q_{max}), water yield (WY) and runoff duration (Rd). Regarding the parameters describing the change of concentration of NO_3^- (ΔC_{NO3}) and TKN (ΔC_{TKN}), a positive correlation was found among these parameters (ΔC_{NO3}, ΔC_{TKN}) and the hydro-meteorological variables rainfall amount (P), rainfall kinetic energy (KE) and magnitude of the event (ΔQ). An inverse relationship was found between ΔC_{TKN} and RL (r = - 0.23, p < 0.01) and K (r = - 0.31, p < 0.01).
290 Finally, the concentrations during runoff events were not controlling factors for the direction of the hysteresis of NO_3 and TKN, but these variables (especially $C_{initial}$) were controlling the hysteresis magnitude for NO_3^- (ΔC_{NO3}) and TKN (ΔC_{TKN}), although in different ways (Table 2). Thus, $C_{initial}$ showed positive correlations with ΔC_{NO3} and negative with ΔC_{TKN}.

Table 2. Pearson correlation coefficients between hysteresis descriptors (ΔR and ΔC) and event characteristics. Values displayed in bold indicates correlation is significant at 0.01 level and italics indicate correlation is significant at 0.05 level.

	Hysteresis direction (ΔR)		Hysteresis magnitude (ΔC)	
	NO_3^-	TKN	NO_3^-	TKN
Antecedent conditions				
AP7d	-0.18	0.09	-0.19	-0.08
AP15d	-0.19	0.16	-0.19	-0.01
Q_b	-0.14	0.12	*-0.22*	0.02
Δt	0.08	0.03	**0.27**	0.05
Event characteristics				
P	*-0.22*	**0.36**	**0.27**	**0.27**
IP10	*-0.24*	0.00	0.05	*0.25*
KE	*-0.24*	**0.32**	*0.24*	**0.31**
Q_{max}	**-0.29**	**0.29**	-0.03	**0.28**
WY	-0.17	**0.38**	-0.08	0.04
ΔQ	-0.06	0.18	**0.29**	**0.35**
RL	0.03	-0.13	0.12	*-0.23*
K	0.10	0.17	-0.03	**-0.31**
Rd	-0.04	**0.37**	0.12	-0.09
Concentrations during the event				
$C_{initial}$	-0.06	0.04	**0.40**	**-0.54**
C_{max}	0.08	0.15	0.16	*0.25*
C_{mean}	-0.14	0.08	0.16	*0.24*

AP7d: accumulated rainfall 7 days before the event; AP15d: accumulated rainfall 15 days before the event; Q_b: discharge at the beginning of the event; P: rainfall amount; IP10: maximum 10-min rainfall intensity; KE: rainfall kinetic energy; Q_{max}: peak discharge; WY: water yield; ΔQ: magnitude of the event; RL: relative length of the rising limb; k: slope of the initial phase of the hydrograph falling limb; Rd: runoff event duration, Δt: time from the previous runoff event; $C_{initial}$: initial concentration; C_{max}: maximum concentration; C_{mean}: mean concentration.

RDA analysis confirmed the Pearson´s correlation results. The first two axes explained 82.3% of total variance in the descriptors in NO_3^- and TKN hysteresis (ΔC_{NO3}, ΔC_{TKN}, ΔR_{NO3}, ΔR_{TKN}), accounting for the first and second canonical axes for 62.4% and 19.9%, respectively. ΔC_{TKN} and ΔR_{TKN} loaded positively in the first axis and pointed in the same direction as rainfall-runoff magnitude variables, indicating a positive relationship with these. ΔC_{TKN} and ΔC_{NO3} loaded negatively in the second axis and pointed in an opposite direction to k, suggesting that an inverse relationship exists between both variables. On the other hand, ΔR_{NO3} loaded negatively in the second axis and pointed in an opposite direction to P and Q_{max}, indicating that an inverse relationship occurs with these variables.
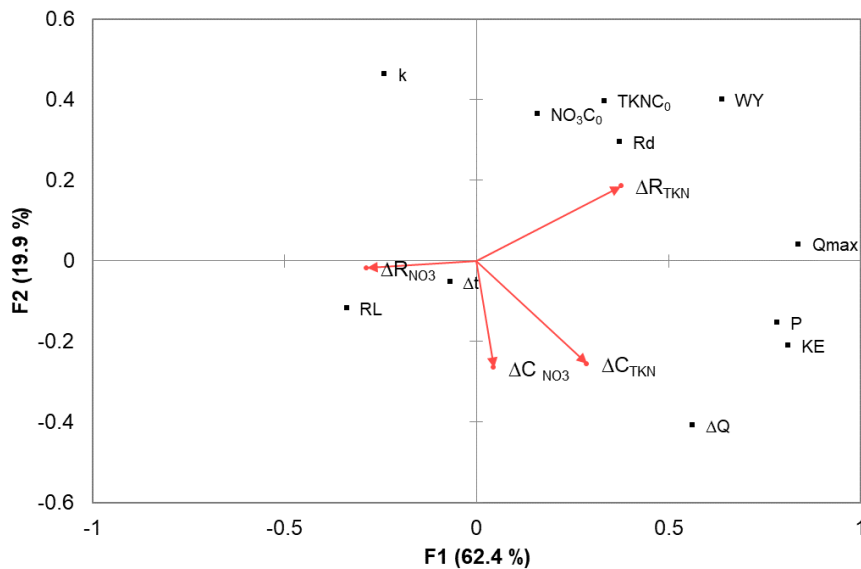
Figure 7: Redundancy analysis distance biplot showing ordinations of explanatory and response variables. P: rainfall amount; KE: rainfall kinetic energy; Qmax: peak discharge; WY: water yield; ΔQ: magnitude of the event; RL: relative length of the rising limb; k: slope of the initial phase of the hydrograph falling limb; Rd: runoff event duration, Δt: time from the previous runoff event; NO_3^- or TKN $C_{initial}$: initial concentration; NO_3^- or TKN C_{max}: maximum concentration. The red arrows are the vectors of the hysteresis descriptors (ΔC_{NO3}, ΔR_{NO3}, ΔC_{TKN}, ΔR_{TKN}).

4 Discussion

High-frequency water quality monitoring facilities identification of C-Q dynamics at the event scale (Lloyd et al., 2016; Vaughan et al., 2017; Rose et al., 2018; Musolff et al., 2021; Winter et al., 2021).   We observed that, in general, the NO_3^- and TKN concentrations increased during runoff events in comparison to pre-event conditions, indicating the predominance of an enrichment response during runoff events and suggesting that the N delivery in the catchments is mainly controlled by diffuse sources. Nitrate concentrations in drinking water in Europe are restricted to 50 mg L^{-1} as NO_3^- or 11.3 mg L^{-1} NO_3^--N (Directive 98/83/EC), and this limit was not exceeded for Corbeira. However, considering that in well-oxygenated surface waters, nitrate levels above 0.5-1.0 mg L^{-1} can pose a risk of water eutrophication (Camargo and Alonso, 2007) and that 2 mg L^{-1} is the threshold identified in the European Nitrogen Assessment as an appropriate target for establishing a river system in good ecological conditions, the data obtained (Table 1) indicate that the study area may be threatened by potential risk of eutrophication due to increased nitrogen concentration. This will clearly have important implications for compliance with water quality targets, and it must be borne in mind that the study area flows into the Abegondo-Cecebre reservoir, a very important source of drinking water for one of the largest cities in the northwest Iberian Peninsula.

4.1 Nitrate and Kjeldahl nitrogen hysteresis patterns

The NO_3^- dynamic during the runoff events was dominated by anticlockwise hysteresis. This pattern suggests that contributors during the falling limb are richer in NO_3^- than during the rising limb and is associated with nitrate transport via groundwater and subsurface flow. Groundwater, which dominates baseflow, contains low NO_3^- concentrations in this catchment. Thus, Rodríguez-Blanco et al., (2015), showed that NO_3^- concentrations in summer (low-flow conditions dominated by groundwater) were lower (around 3.75 mg L^{-1}) than those measured in winter (5.67 mg L^{-1}). On the other hand, the soils of the study area have high infiltration rates (Taboada-Castro et al., 1999) and much of streamflow comprises water leached through the soil profile (Rodríguez-Blanco et al., 2019), so subsurface flow is a likely pathway delivering additional NO_3^- during runoff events. In fact, in the events showing anticlockwise loops, the maximum NO_3^- concentrations in the stream were registered after peak discharge (Figure 5a, b) when the contribution of subsurface flow to streamflow (estimated from the hydrograph separation method with electrical conductivity as a tracer) is maximum, and then decreases as the subsurface recedes. This could also be related to the higher availability of NO_3^- in the shallow soil horizon than in deeper groundwater, arguably because of mineralization of organic matter and the mineral and organic fertilizer applied to agricultural soils in the catchment, as demonstrated by both modelling and data-driven approaches (López Periago et al., 2002). Other authors, however, have attributed anticlockwise hysteresis to a particular spatial distribution of the sources. Thus, Vaughan et al. (2017) linked this pattern to the transport of proximal sources at the beginning of runoff events, followed by enrichment from distal and substantial sources of nitrate, which seems not to be the case in the study catchment. While enrichment with anticlockwise rotation was the dominant pattern for NO_3^- in the study catchment, some events exhibited enrichment patterns but with clockwise hysteresis (Figure 5 and 6), indicating a higher NO_3^- concentration in the rising limb of the hydrograph than in the falling limb. This pattern was mainly observed in small spring events occurring in 2008 and 2009 and could be attributed to the transport of NO_3^- from near-stream areas recently fertilizers.

The dominance of anticlockwise nitrate hysteresis with higher concentrations on the falling limb of the hydrograph is line with findings from reported studies conducted in forest and agricultural catchments (Outram et al., 2016; Andrea et al., 2006; Cerro et al., 2014; Musolff et al., 2021). However, they contrast with interpretations presented in several previous studies carried out in rural catchments, which described exclusively NO_3^- dilution processes linked to dilution of NO_3^- concentrations in groundwater by surface runoff (D'Amario et al., 2021; Bowes et al., 2015; Aguilera and Melack, 2018; Rose et al., 2018a) or the exhaustion of a finite pool of NO_3^- in the riparian zone and shallow groundwater (Koenig et al., 2017; Duncan et al., 2017). However, in the study catchment, the dilution responses (with anticlockwise rotation ($\Delta C \leq 0\%$)) were only observed in certain larger runoff events associated with wet antecedent conditions, short interarrival time ($\Delta t < 1$ hour) and larger event-water contribution (Rodríguez-Blanco et al., 2015) . A possible reason for the initial dilution of the concentrations could be the preceding wetting of the catchment which favors the delivery of relatively low-nitrate water flushed to the stream from low-NO_3^- concentration sources, such as direct rainfall (mean NO_3^- concentrations determined in rainwater samples = 0.1 mg NO_3^- L^{-1}, Rodríguez-Blanco et al., 2015) to the stream and runoff from roads and paved area, as has been observed in other headwater

streams (Poor and McDonnell 2007; Kato et al., 2009). Following the initial dilution, concentrations increased above pre-event values, reaching the highest NO_3^- concentrations after maximum discharge. The return of NO_3^- concentrations to the values before the rainfall-runoff event is especially slow in these events (Figure 5b) and NO_3^- concentrations remain elevated for several days until streamflow returns to baseflow.

365 Mechanisms responsible for TKN mobilization differ from those mobilizing NO_3^-. Thus, a clockwise enrichment pattern for TKN concentration was dominant for most events (Figure 5d), suggesting a delivery of TKN to the stream network via fast pathways from proximal sources or relatively easily connected to the stream as event discharge increases, with possible rapid exhaustion of the material to be transported (Creed et al., 2015). The TKN response was almost concurrent with discharge, which leads to thinking that TKN may come from the eroded soil and litter layer delivered to the stream primarily by surface

370 runoff, in a similar way to suspended sediment matter and particulate phosphorus (Rodríguez-Blanco et al., 2013; 2019). These results generally agree with many that also reported clockwise organic nitrogen hysteresis patterns (Vanderbilt et al., 2003; Inamdar and Mitchell, 2006; Rose et al., 2018; D'Amario et al., 2021). In contrast, Hagedorn et al. (2000) observed anticlockwise hysteresis for organic nitrogen in a forest catchment in Switzerland due to the mobilization of its passage through the forest canopy and organic-rich topsoil. Others have attributed this pattern (anticlockwise) to distant source areas activated

375 later in the runoff events as hydrological pathways connect (Aguilera and Melack, 2018). In the study area, this pattern was only observed during some low magnitude events (20 of 26, P < 16 mm) recorded in spring and summer, so it is highly unlikely to come from distant sources. Rather, given the event characteristics (low magnitude rainfall-runoff events with low particulate material), the presence of anticlockwise hysteresis could be indicative of a large proportion of dissolved fraction in TKN, which passes through the soil and subsequently enters the stream by subsurface flow.

380 Hysteresis patterns may vary among events and antecedent soil moisture conditions are often recognized as an important factor in the response of different constituent concentrations among events, even when rainfall characteristics are approximately similar (Butturini et al., 2006; Guarch-Ribot and Butturini, 2016; Baker and Showers, 2019). However, other authors have highlighted the significant role played by rainfall-runoff events characteristic of hysteresis patterns (Lloyd et al., 2016; Chen et al., 2012). For example, (Chen et al., 2012) emphasized the role of the runoff event magnitude influencing the magnitude

385 and rotation direction of the hysteresis patterns, whereas Lloyd et al., (2016) underlined the combined effect exerted by storm duration, maximum discharge during the runoff event and the time elapsing from the previous runoff events on controlling N hysteresis magnitude and rotation. In this catchment, hysteresis direction and magnitude for TKN were better explained by event characteristics, such as rainfall, peak discharge, and event magnitude than by antecedent rainfall and baseflow. Thus, the hysteresis magnitude value was dependent on the magnitude of the hydrological response of the catchment and the delivery of

390 particulate material to the stream. In the catchment, the main sediment supply to the stream is associated with the erosion of cultivated soil with high connectivity to the stream, which favors the quick delivery of particulate material to the stream. The results obtained for TKN are consistent with the findings obtained for suspended sediments, phosphorus, and particulate metals in the study area by Rodríguez-Blanco et al. (2010, 2013, 2018), showing that the sources of material particulate are close to the monitoring station, which may explain the prevalence of clockwise hysteresis for TKN. For NO_3^- hysteresis patterns the

395 role of hydrometeorological conditions were more complex and dynamics should be controlled by biogeochemical processes coupled with hydrological processes. In fact, the NO_3^- hysteresis magnitude (ΔC) was related to the magnitude of the event (ΔQ) and the time elapsed since a preceding runoff event (Δt), which should favour the build-up of NO_3^-.

Overall, the results show that it was possible to understand the transport of N and the mechanism controlling in a rural temperate humid environment. These insights could be useful for implementing mitigation techniques to prevent water quality

400 degradation in the context of increasing human and climate perturbations. Thus, to minimize nitrate delivery to streams, catchment management should focus on reducing N stores in the soil, whereas for protecting water quality against for TKN, practices that may reduce the supply of water by surface runoff and sediment are also required, because they seem to be the main responsible for TKN transport in this region. More event-based observations are needed to better clarify the mechanism of the N delivery process.

405 **5 Conclusion**

Our study uses measurements of stream discharge and nitrogen (NO_3^- and TKN) obtained by intensive sampling to investigate the nitrogen concentration dynamics at event scale. The results show the potential of high-frequency N concentration monitoring to advance our understanding of coupled hydrological and biogeochemical systems in the context of contrasting hydrometeorological conditions. The assessment of nitrogen C-Q relationships and their controlling factors has provided

410 evidence of the different NO_3^- and TKN dynamics during the runoff events, suggesting the presence of distinct delivery mechanisms and differences in dominant hydrological pathways. NO_3^- behaviour during the runoff events was dominated by anticlockwise hysteresis, whereas clockwise hysteresis prevailed in the TKN dynamic.

The divergence dynamics observed between N components in the study area highlights the need to understand the transport of N and the mechanism controlling for the implementation of future water quality monitoring programs and for the development

415 of N-specific management plans to ensure that control measures are most effective at the catchment scale, specially within the context of increasing nitrate concentrations, a pressing environment issue.

Acknowledgements

This research was carried out within the projects REN2003-08143, funded by the Spanish Ministry of Education and Science, and PGIDIT05RAG10303PR and 10MDS103031PR, financed by the Xunta of Galicia.

420

References

Abbott, B.W., Bishop, K., Zarnetske, J.P., Minaudo, C., Chapin F.S., Drause, S., Hannah, D.M., Conner, L., Ellison, D., Godsey, S.E., Plont, S., Marçais, J., Kolbe, T., Huebner, A., Frei, R.J., Hampton, T., Gu, S., Buhman, M., Sayedi, S.S., Ursache, O., Chapin, M., Henderson, K.D., Pinay, G.: Human domination of the global water cycle absent from depictions and perceptions, Nat. Geosci., 12, 533-540, doi:10.1038/s41561-019-0374-y, 2019.

Aguilera, R. and Melack, J. M.: Concentration-discharge responses to storm events in Coastal California Watersheds, Water Resour. Res., 54, 407–424, doi:10.1002/2017WR021578, 2018.

APHA. 1998. Standard Methods for Examination of Water and Wastewater. APHA: Washington.

Ameijenda, C. Integrated management of water resources and its application to local planning of the Abegondo Cecebre 07/ENV/E/0826 LIFE+project. Spanis J Rural Develop., 1, 35-40, doi:10.5261/2010.ESP1.02, 2010

Baker, E. B. and Showers, W. J.: Hysteresis analysis of nitrate dynamics in the Neuse River, NC, 652, Scie. Totl Environ., doi:10.1016/j.scitotenv.2018.10.254, 2019.

Bieroza, M. Z. and Heathwaite, A. L.: Seasonal variation in phosphorus concentration-discharge hysteresis inferred from high-frequency in situ monitoring, J. Hydrol., 524, doi:10.1016/j.jhydrol.2015.02.036, 2015.

Bieroza, M. Z., Heathwaite, A. L., Bechmann, M., Kyllmar, K., and Jordan, P.: The concentration-discharge slope as a tool for water quality management, Scie. Total Environ., 630, 738–749, doi:10.1016/J.SCITOTENV.2018.02.256, 2018.

Bowes, M. J., Jarvie, H. P., Halliday, S. J., Skeffington, R. A., Wade, A. J., Loewenthal, M., Gozzard, E., Newman, J. R., and Palmer-Felgate, E. J.: Characterising phosphorus and nitrate inputs to a rural river using high-frequency concentration-flow relationships, Scie. Total Environn., 511, doi:10.1016/j.scitotenv.2014.12.086, 2015.

Burns, D. A., Pellerin, B. A., Miller, M. P., Capel, P. D., Tesoriero, A. J., and Duncan, J. M.: Monitoring the riverine pulse: Applying high-frequency nitrate data to advance integrative understanding of biogeochemical and hydrological processes, WIRES Water, 6, doi:10.1002/wat2.1348, 2019.

Butturini, A., Francesc, G., Jérôme, L., Eusebi, V., and Francesc, S.: Cross-site comparison of variability of DOC and nitrate c-q hysteresis during the autumn-winter period in three Mediterranean headwater streams: A synthetic approach, Biogeochemistry, 77, doi:10.1007/s10533-005-0711-7, 2006.

Butturini, A., Alvarez, M., Bernał, S., Vazquez, E., and Sabater, F.: Diversity and temporal sequences of forms of DOC and NO3- discharge responses in an intermittent stream: Predictable or random succession?, J. Geophys. Res. Biogeosci., 113, doi:10.1029/2008JG000721, 2008.

Camargo, J.A., Alonso, A.: Contaminación por nitrógeno inorgánico en los ecosistemas acuáticos: problemas medioambientales, criterios de calidad del agua, e implicaciones del cambio climático, Ecosistemas, 16, 98-110, 2007.

Cerro, I., Sanchez-Perez, J. M., Ruiz-Romera, E., and Antigüedad, I.: Variability of particulate (SS, POC) and dissolved (DOC, NO$_3$) matter during storm events in the alegria agricultural watershed, Hydrol. Process., 28, doi:10.1002/hyp.9850, 2014.

Cey, E.E., Rudolph, D.L., Parkin, G.W., Aravena, R.: Quantifying groundwater discharge to a small perennial stream in southern Ontario, Canada. J. Hydrol., 210, 21–37, doi:10.1016/S0022-1694(98)00172-3, 1998.

455 Chen, N., Wu, J., and Hong, H.: Effect of storm events on riverine nitrogen dynamics in a subtropical watershed, southeastern China, Scie. Total Environ., 431, doi:10.1016/j.scitotenv.2012.05.072, 2012.

Creed, I. F., Mcknight, D. D. M., Pellerin, B. A., Green, M. B., Bergamaschi, B. A., Aiken, G. R., et al. (2015). The river as a chemostat: Fresh perspectives on dissolved organic matter flowing down the river continuum. Can. J. Fish. Aquat. Sci., 14, 1–1285, doi:10.1139/cjfas-2014-0400

460 D'Amario, S. C., Wilson, H. F., and Xenopoulos, M. A.: Concentration-discharge relationships derived from a larger regional dataset as a tool for watershed management, Ecol. Appl., doi:10.1002/eap.2447, 2021.

Dupas, R., Jomaa, S., Musolff, A., Borchardt, D., and Rode, M.: Disentangling the influence of hydroclimatic patterns and agricultural management on river nitrate dynamics from sub-hourly to decadal time scales, Scie. Total Environ., 571, doi:10.1016/j.scitotenv.2016.07.053, 2016.

465 EC (European Comision) 2019. Informe de la comisión al parlamento europeo y al consejo sobre la aplicación de la directiva marco sobre el agua (2000/60/ce) y la directiva sobre inundaciones (2007/60/ce) segundos planes hidrológicos de cuenca primeros planes de gestión del riesgo de inundación. SWD 42. 234 pp.

EEA, 2018. European waters -- Assessment of status and pressures 2018. 90 pp.

Eludoyin, A. O., Griffith, B., Orr, R. J., Bol, R., Quine, T. A., and Brazier, R. E.: An evaluation of the hysteresis in chemical 470 concentration–discharge (C–Q) relationships from drained, intensively managed grasslands in southwest England, Hydrol. Scie. J., 62, 1243–1254, doi:10.1080/02626667.2017.1313979, 2017.

EU (European Union): 1998, Directive 98/83/CE relative to human drinking water quality, Official Journal of European Communities L330.

EU (European Union): 2000, Directive 2000/60/CE of the European Parliament and of the Council establishing a framework 475 for community action in the field of water policy, Official Journal of European Communities L327.

Evans, C., and Davies, T. D.: Causes of concentration/discharge hysteresis and its potential as a tool for analysis of episode hydrochemistry, Water Resour. Res., 34(1), 129–137, doi: 10.1029/97WR01881, 1998.

Hagedorn, F., Schleppi, P., Waldner, P., and Flühler, H.: Export of dissolved organic carbon and nitrogen from Gleysol dominated catchments - The significance of water flow paths, Biogeochemistry, 50, doi:10.1023/A:1006398105953, 2000.

480 Hewlett JD, Hibbert AR.: Factor affecting the response of small watersheds to precipitation in humid areas. In Forest Hydrology, Sopper WE, Lull HW (eds). Pergamon: NY; 275–290, 1967.

IGME (Instituto Tecnológico Geominero de España), 1981. Mapa Geológico de España, 1:50,000. Hoja 45. Betanzos. Spain.

Inamdar, S. P. and Mitchell, M. J.: Hydrologic and topographic controls on storm-event exports of dissolved organic carbon (BOC) and nitrate across catchment scales, Water Resour. Res., 42, doi:10.1029/2005WR004212, 2006.

485 Kato, T., Kuroda, H., and Nakasone, H.: Runoff characteristics of nutrients from an agricultural watershed with intensive livestock production, J. Hydrol., 368, doi:10.1016/j.jhydrol.2009.01.028, 2009.

IUSS Working Group WRB. 2014. World Reference Base for Soil Resources. 2014. International soil classification system for naming soils and creating legends for soil maps. World Soil Resources Reports. No 106. Rome. FAO.

Kaushal, S. S. and Lewis, W. M.: Patterns in the chemical fractionation of organic nitrogen in Rocky Mountain streams,
490   Ecosystems, 6, doi:10.1007/s10021-003-0175-3, 2003.

Knapp, J. L. A., von Freyberg, J., Studer, B., Kiewiet, L., and Kirchner, J. W.: Concentration-discharge relationships vary among hydrological events, reflecting differences in event characteristics, Hydrol. Earth Syst. Sci., 24, 2561–2576, doi:10.5194/HESS-24-2561-2020, 2020.

Legendre, P., Legendre, L.: Numerical ecology. Elsevier: Amsterdam, 2012.

495   Linsley, R.K., Kohler, M.A., Paulhus, J.C. 1949. Applied hydrology. McGraw-Hill Book Co., New York.

Lloyd, C. E. M., Freer, J. E., Johnes, P. J., and Collins, A. L.: Using hysteresis analysis of high-resolution water quality monitoring data, including uncertainty, to infer controls on nutrient and sediment transfer in catchments, Sci. Total Environ., 543, doi:10.1016/j.scitotenv.2015.11.028, 2016.

Martínez-Santos, M., Antigüedad, I., and Ruiz-Romera, E.: Hydrochemical variability during flood events within a small
500   forested catchment in Basque Country (Northern Spain), Hydrol. Process., 28, doi:10.1002/hyp.10011, 2014.

Meybeck, M.: Looking for water quality, Hydrol. Process., 19, 331-338, doi:10.1002/hyp.5778, 2005.

Nolan, K. M. and Hill, B. R.: Storm-runoff generation in the Permanente Creek drainage basin, west central California - An example of flood-wave effects on runoff composition, J. Hydrol., 113, doi:10.1016/0022-1694(90)90183-X, 1990.

Outram, F. N., Cooper, R. J., Sünnenberg, G., Hiscock, K. M., and Lovett, A. A.: Antecedent conditions, hydrological
505   connectivity and anthropogenic inputs: Factors affecting nitrate and phosphorus transfers to agricultural headwater streams, Sci. Total Environ., 545–546, doi:10.1016/j.scitotenv.2015.12.025, 2016.

Pellerin, B.A., Wollheim, W.M., Feng, X., Vörsmarty, C.J.: The application of electrical conductivity as a tracer for hydrograph separation in urban catchments. Hydrol. Process., 22, 1810-1818, doi:10.1002/hyp.6786

Poor, C. J. and McDonnell, J. J.: The effects of land use on stream nitrate dynamics, J. Hydrol., 332,
510   doi:10.1016/j.jhydrol.2006.06.022, 2007.

Ramos, T. B., Gonçalves, M. C., Branco, M. A., Brito, D., Rodrigues, S., Sánchez-Pérez, J. M., Sauvage, S., Prazeres, Â., Martins, J. C., Fernandes, M. L., and Pires, F. P.: Sediment and nutrient dynamics during storm events in the Enxoé temporary river, southern Portugal, catena, 127, doi:10.1016/j.catena.2015.01.001, 2015.

Rodríguez-Blanco, M. L., Taboada-Castro, M. M., and Taboada-Castro, M. T.: Rainfall-runoff response and event-based
515   runoff coefficients in a humid area (northwest Spain), Hydrol. Sci. J., 57, doi:10.1080/02626667.2012.666351, 2012.

Rodríguez-Blanco, M. L., Taboada-Castro, M. M., and Taboada-Castro, M. T.: Phosphorus transport into a stream draining from a mixed land use catchment in Galicia (NW Spain): Significance of runoff events, J. Hydrol., 481, doi:10.1016/j.jhydrol.2012.11.046, 2013.

Rodríguez-Blanco, M. L., Taboada-Castro, M. M., Taboada-Castro, M. T., and Oropeza-Mota, J. L.: Relating nitrogen export patterns from a mixed land use catchment in NW Spain with rainfall and streamflow, Hydrol. Process., 29, doi:10.1002/hyp.10388, 2015.

Rodríguez-Blanco, M. L., Taboada-Castro, M. M., and Taboada-Castro, M. T.: An overview of patterns and dynamics of suspended sediment transport in an agroforest headwater system in humid climate: Results from a long-term monitoring, Scie. Total Environ., 648, doi:10.1016/j.scitotenv.2018.08.118, 2019.

Rodríguez-Blanco, M. L., Taboada-Castro, M. M., and Taboada-Castro, M. T.: An assessment of the recent evolution of the streamflow in a near-natural system: A case study in the headwaters of the mero basin (galicia, Spain), Hydrol., 7, doi:10.3390/hydrology7040097, 2020.

Rose, L. A., Karwan, D. L., and Godsey, S. E.: Concentration–discharge relationships describe solute and sediment mobilization, reaction, and transport at event and longer timescales, Hydrol. Process., 32, 2829–2844, doi:10.1002/hyp.13235, 2018.

Taboada-Castro, M.M., Lado, M., Diéguez-Villar, A., Paz-González, A.: Evolución temporal de la infiltración superficial a escala de parcela. Jornadas Internacionales sobre Erosión Hídrica, Coruña, 1998.

Vanderbilt, K. L., Lajtha, K., and Swanson, F. J.: Biogeochemistry of unpolluted forested watersheds in the Oregon Cascades: Temporal patterns of precipitation and stream nitrogen fluxes, Biogeochemistry, 62, doi:10.1023/A:1021171016945, 2003.

Vörösmarty, C. J., McIntyre, P. B., Gessner, M. O., Dudgeon, D., Prusevich, A., Green, P., Glidden, S., Bunn, S. E., Sullivan, C. A., Liermann, C. R., Davies, P. M.: Global threats to human water security and river biodiversity, Nature, 467, 555-561, doi: 10.1038/nature09440, 2010.

Winter, C., Lutz, S. R., Musolff, A., Kumar, R., Weber, M., and Fleckenstein, J. H.: Disentangling the impact of catchment heterogeneity on nitrate export dynamics from event to long-term time scales, Water Resour. Res., 57, doi:10.1029/2020WR027992, 2021.